CRYSTAL GROWTH & DESIGN
2008
VOL. 8, NO. 8
2990–2994

Surface-Assisted Synthesis of Microscale Hexagonal Plates and Flower-like Patterns of Single-Crystalline Titanium Disulfide and Their Field-Emission Properties

You-Rong Tao, Xing-Cai Wu,* Yu-Ling Zhang, Lin Dong, Jun-Jie Zhu, and Zheng Hu

Key Laboratory of Mesoscopic Chemistry of MOE, State Key Laboratory of Coordination Chemistry, and School of Chemistry and Chemical Engineering, Nanjing University, Nanjing 210093, P. R. China

Received January 30, 2008; Revised Manuscript Received May 10, 2008

ABSTRACT: Microscale hexagonal plates of single-crystalline TiS_2 with a border length of about 7.8 μm and thickness of about 156 nm were grown on Ti substrate by a facile surface-assisted chemical-vapor-transport approach at 550 °C. The TiS_2 plates (petals) and Ti particles (flower center) constituted flower-like patterns when the reaction temperature was at 650−750 °C. The surface of the Ti foils was completely converted into TiS_2 microplates with a thickness of 100−400 nm when the reaction temperature reached 850 °C. The growth mechanism was briefly discussed. Preliminary field-emission experiments using the samples obtained at 550, 650, and 850 °C as cold electron cathodes showed that the materials have a notable emission current, and their turn-on fields, defined as the electric field required to produce a current density of 10 μA/cm^2, are 11.5, 16.3, and 19.5 V/μm, respectively, suggesting their potential application in electron emission devices.

1. Introduction

There is growing interest in fabricating micro/nanostructures on metal or semiconductor wafers to form novel "functional building blocks". For example, boron nitride microcones[1] and molybdenum and molybdenum oxides nanowires[2] vertically grown on silicon substrates have been used as electronic field emitters, and zinc oxides nanowires vertically grown on sapphire substrates have been used as ultraviolet nanolasers.[3] Thermal evaporation or chemical vapor deposition is particularly simple and useful for producing the micro/nanostructures, but a surface-assisted chemical-vapor-transport (CVT) approach is another optional cost-effective route.

Titanium disulfide (TiS_2) crystallizes in a layered (1T) structure, where the layers of TiS_2 are stacked together via the relatively weak van-der-Waals forces. Each TiS_2 layer contains a metal layer sandwiched between two chalcogen layers with the metal in an octahedral coordination mode.[4] Some band-structure calculations indicate that TiS_2 is a narrow-gap ($\sim$ 0.2 eV) semiconductor,[5] or semimetal.[6] In fact, some physical measurements exhibit either semimetallic[7] or semiconducting[8] behavior due to a strong tendency toward nonstoichiometry with titanium excess. Resistivity measurements in highly stoichiometric TiS_2 reveal a metallic behavior at all temperatures with an unusual T^2 temperature relationship,[9,10] while Hall coefficient and thermoelectric power measurements support the semiconducting hypothesis.[11] Owing to its layered structure, TiS_2 can form intercalation compounds with a wide variety of guest species,[12–14] and serve as cathode materials in secondary batteries.[15,16] The type and concentration of the intercalated species usually have a great effect on the physical properties of the host;[17–19] for instance, the thermal conductivity of TiS_2 through Bi intercalation decreases remarkably,[20] and TiS_2 intercalated with Fe, Co, and Ni elements shows low-dimensional magnetic ordered structures at low temperature.[21] In recent years, a few TiS_2 nanostructures have been reported such as TiS_2 nanotubes,[22] lithium-intercalated TiS_2 nanotubes,[23] TiS_2 nanowire arrays,[24] and two-dimensional nanocrystalline islands of TiS_2.[25] It shows that TiS_2 is noticed again. However, controlled organization into flower-like microstructures from plate-like building blocks remains a challenge. Such a capability is attractive to scientists not only because of its importance in

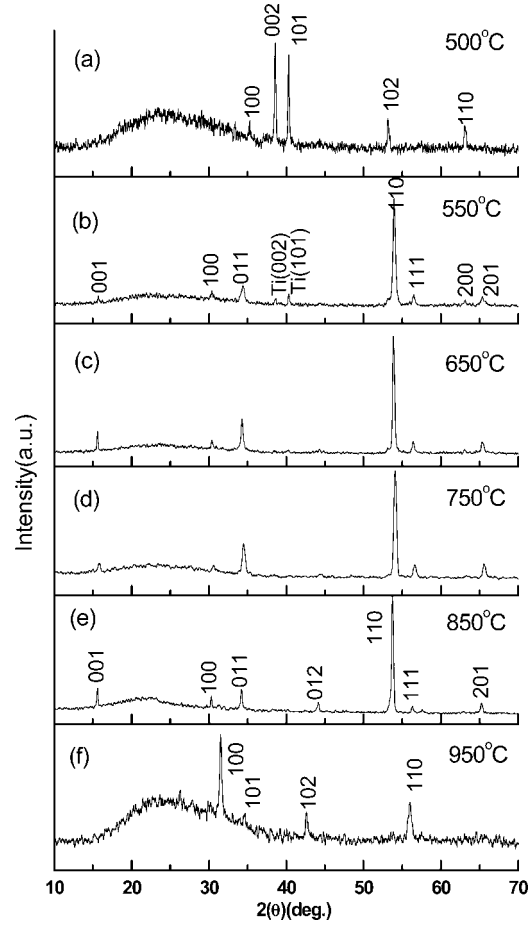

Figure 1. Powder XRD patterns of TiS_2 microstructures on the substrates obtained at (a) 500 °C, (b) 550 °C, (c) 650 °C, (d) 750 °C, (e) 850 °C, and (f) 950 °C. Impure peaks can be attributed to Ti on the substrate.

* Author to whom correspondence should be addressed. Fax: +86-25-83317761. E-mail: wuxingca@netra.nju.edu.cn.

10.1021/cg800113n CCC: $40.75
Published on Web 07/03/2008

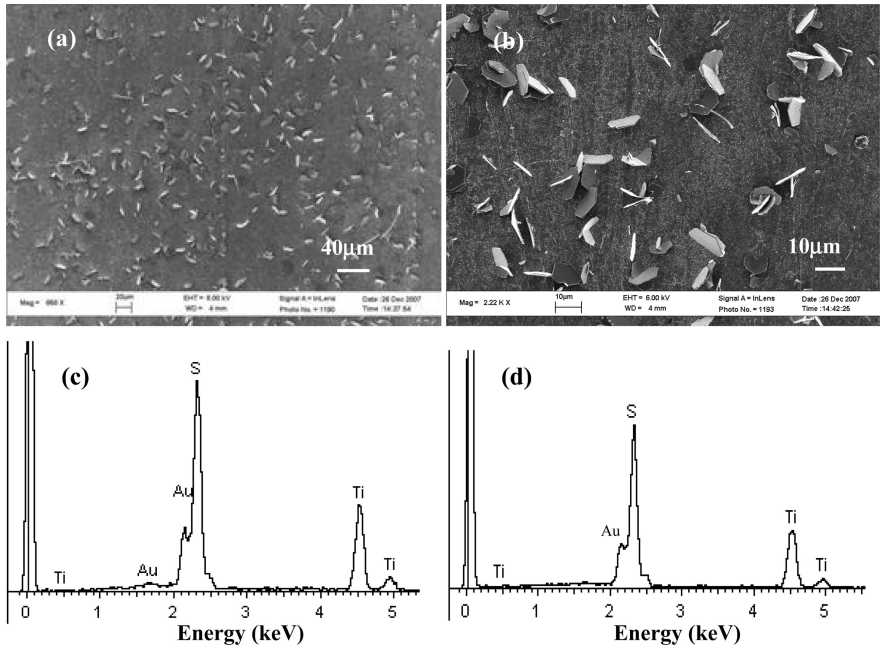

Figure 2. (a, b) SEM images of TiS_2 microstructures prepared at 550 °C (LEO-1530VP), (c) EDX spectrum of TiS_2 microplate obtained at 550 °C, and (d) EDX spectrum of the surface of the substrate after the reaction finished at 550 °C.

constructing building blocks but also for its great potential applications. Herein, a surface-assisted CVT approach was applied in the growth of microscale plates and flower-like patterns of TiS_2 on Ti substrate; their field emission (EF) performances also were measured.

2. Experimental Procedures

In the experiments, titanium (Ti) foils (99.9%, 0.2 × L × L mm) and sulfur (S) powders (99.8%) were used. Three pieces of Ti foils with a size of ca. 0.2 × 5 × 10 mm (134.0 mg) and S powders (8.98 mg) were sealed in a quartz ampule under a vacuum (Φ6 mm × 13 mm, ca. 10^{-2} Pa). The ampule was placed in a conventional horizontal furnace with a temperature gradient of ca. 10 K cm^{-1} from center to edge, and the end with Ti foils was put at the center of the furnace, and then heated at different temperatures (500, 550, 650, 750, 850, and 950 °C) for 30 min; finally, TiS_2 microstructures were grown on Ti foils. After the furnace was cooled to room temperature, the foils with TiS_2 micro/nanostructures were extracted from the quartz ampule.

The products were characterized by an X-ray diffractometer ((XRD; Shimadzu XRD-6000) with graphite monochromatized Cu Kα-radiation, scanning electron microscope (SEM; JEOL-JEM-6360LV and LEO-1530VP) with energy-dispersive X-ray spectrometer (EDX), and high-resolution electron microscopy with a point resolution of 0.19 nm (HRTEM; JEOL model JEM-2100). The electron field emission measurement were performed by using parallel-plate configuration with a space of 225 μm in a vacuum chamber at a pressure of 5.0×10^{-4} Pa at room temperature. A dc voltage sweeping from 0 to 4800 V was applied to the sample.

3. Results and Discussion

Structure and Morphology. Figure 1 shows the powder X-ray diffraction (XRD) patterns of as-prepared products at different temperatures. Figure 1a indicates the reflection peaks of the products obtained at 500 °C, which can be indexed as the hexagonal phase of Ti (JCPDS File 44-1294). It reveals that Ti does not react with S below 500 °C. Figure 1, panels b−e exhibit the reflection peaks of the products obtained at 550−850 °C, which can be indexed as the hexagonal phase of TiS_2 (JCPDS File 74-1141). Peaks of impurities can be attributed to Ti on wafers. Figure 1f indicates the reflection peaks of the products obtained at 950 °C, which can be indexed as the hexagonal phase of TiS (JCPDS File 12-0534). Therefore, the XRD patterns demonstrate that well-crystallized TiS_2 were obtained at 550−850 °C.

Figure 2a,b are SEM images of the TiS_2 microstructure obtained at 550 °C, which show that hexagonal plates with a border length of about 7.8 μm and thickness of 156 nm were vertically or obliquely grown on Ti substrate along a tip. The EDX spectrum of a single hexagonal plate shown in Figure 2c demonstrates that the molar ratio of Ti and S is 1:1.9, which is close to the standard stoichiometric composition. Figure 2d is EDX spectrum of the surface of the substrate, showing that the molar ratio of Ti and S is 1:1.9, too, so we think that the products on the surface still are TiS_2. Figure 3, panels a,b are SEM images of the TiS_2 microstructure obtained at 650 °C, showing that the microstructures are flower-like patterns with a diameter of about 71 μm. The patterns consist of hexagonal plates of TiS_2 with a border length of about 4.4 μm and thickness of about 400 nm as petals, and flower centers with a diameter of about 9 μm. EDX spectra shown in Figure 3c,d demonstrate that the flower centers and the petals (microplates) are composed of Ti and TiS_2 (the molar ratio of Ti and S is 1:1.8), respectively. Figure 3e is the HRTEM image of a flower petal, and fringe space of 0.25 and 0.28 nm corresponds to the (011) and (100) planes, respectively, which further confirms that the petal is crystallite TiS_2. Figure 3f shows the curves of linear scanning of the flower-like pattern obtained at 750 °C.

Figure 4, panels a and b are SEM images of the TiS_2 microstructure obtained at 750 °C, which shows that the microstructures are also flower-like patterns with a diameter of about 40 μm. The patterns are composed of hexagonal plates (petals) of TiS_2 with a border length of about 9 μm and thickness of about 260 nm, and flower centers with diameter of about 25 μm. EDX spectra shown in Figure 4c,d further demonstrate that the components of the flower centers and the petals are Ti and TiS_2 (the molar ratio of Ti and S is 1: 2.1), respectively. The curves of linear scanning of the flower-like pattern further confirm that flower center is Ti (Figure 3f). Figure 4e is the

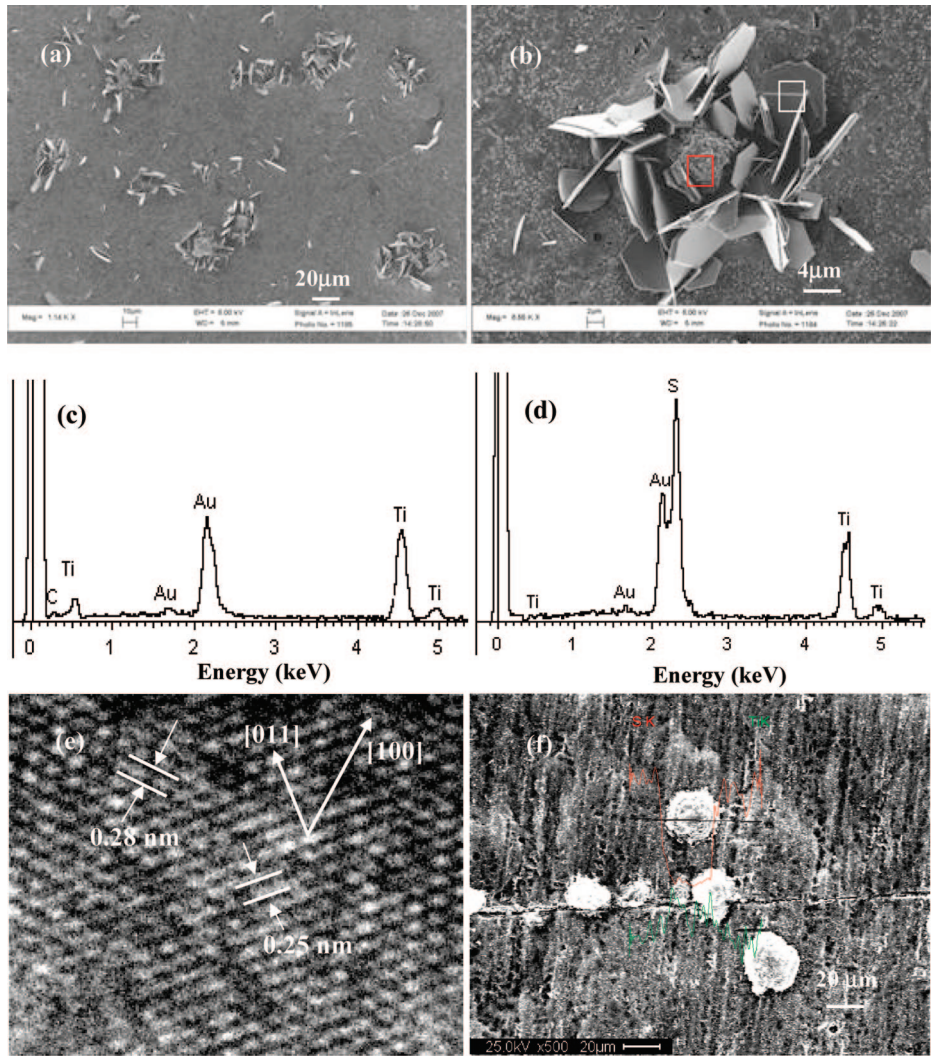

Figure 3. (a, b) SEM images of TiS_2 flower-like patterns prepared at 650 °C (LEO-1530VP). (c) EDX spectrum of the flower center (red box). (d) EDX spectrum (white box) and (e) HRTEM image of the flower petal (hexagonal plate). (f) Linear scan pattern of TiS_2 flower-like patterns prepared at 750 °C (JEOL-JEM-6360LV).

SEM image of the microstructure obtained at 850 °C, which shows that the surface is completely converted into standing microplates of TiS_2 with a thickness of 10−400 nm. The EDX spectrum (Figure 4g) demonstrates that the molar ratio of Ti and S is 1:2.0, so the hexagonal plates are TiS_2. Figure 4f is an SEM image of the microstructure obtained at 950 °C, which shows that the surface with TiS_2 is converted into porous TiS thin films. The EDX spectrum (Figure 4h) reveals that the molar ratio of Ti and S of the thin film is 1:1.2, which supports above XRD results.

Growth Mechanism. The synthesis process does not involve any catalysis, and the microplates are standingly grown on the substrate along the [110] direction (a tip), so the vapor-solid growth process may be the dominating mechanism in our case.[26] When the reaction temperature reaches 550 °C, sulfur (bp 444.6 °C) is evaporated into gas shape, and deposits on the Ti substrate. Then titanium reacts with sulfur vapors, and forms unstable TiS_x into the gas phase. TiS_x in the vapor phase reacts with S vapor, and condenses again on the Ti substrates to form stable TiS_2 seeds. In the following process, TiS_x and S in the vapor phase may have combined with TiS_2 seeds to form TiS_2 microplates (Figure 5a). Owing to the inducement of the seeds, TiS_2 microplates almost stand on the surface of the substrates, similar to the growth of MoO_2 nanorod arrays on Si substrates in a little oxygen.[2] Figure 5b depicts the morphology and growth direction of TiS_2 microplates. When the reaction temperatures are between 650 and 750 °C, the reaction rate rapidly increases to form a few microscale islands of Ti, and then TiS_2 deposits around islands to form flower-like patterns of TiS_2 with a Ti flower center (Figure 5c). When the reaction temperature is 850 °C, the reaction rate further increases so that surface Ti on the substrate all forms TiS_2 microplates. When the reaction temperature reaches 950 °C, TiS_2 microplates are decomposed into porous TiS films.

Electronic Field Emission. The emission current−voltage characteristics were analyzed by using the Fowler−Nordheim (FN) equation for the field emission: $J=(AE^2\beta^2/\Phi)\exp(-B\Phi^{3/2}/E\beta)$, where J is the current density (A/m^2), E ($= V/d$) is the applied field, $B = 6.83 \times 10^9$ ($eV^{-3/2}V\ m^{-1}$), $A = 1.56 \times 10^{-10}$ (AV^{-2} eV), β is a field enhancement factor, and Φ is the work function.[27] Figure 6a depicts the plots of the emission current density (J) as a function of applied field (E) of the products obtained at 550, 650, and 850 °C. Here, we define the turn-on field as the electric field required to produce a current density of 10 $\mu A/cm^2$. Their turn-on fields are 11.5, 16.3, and 19.5 V/μm, respectively. Field emission (FE) is a physical phenomenon of quantum tunneling, during which electrons are injected from a material surface into

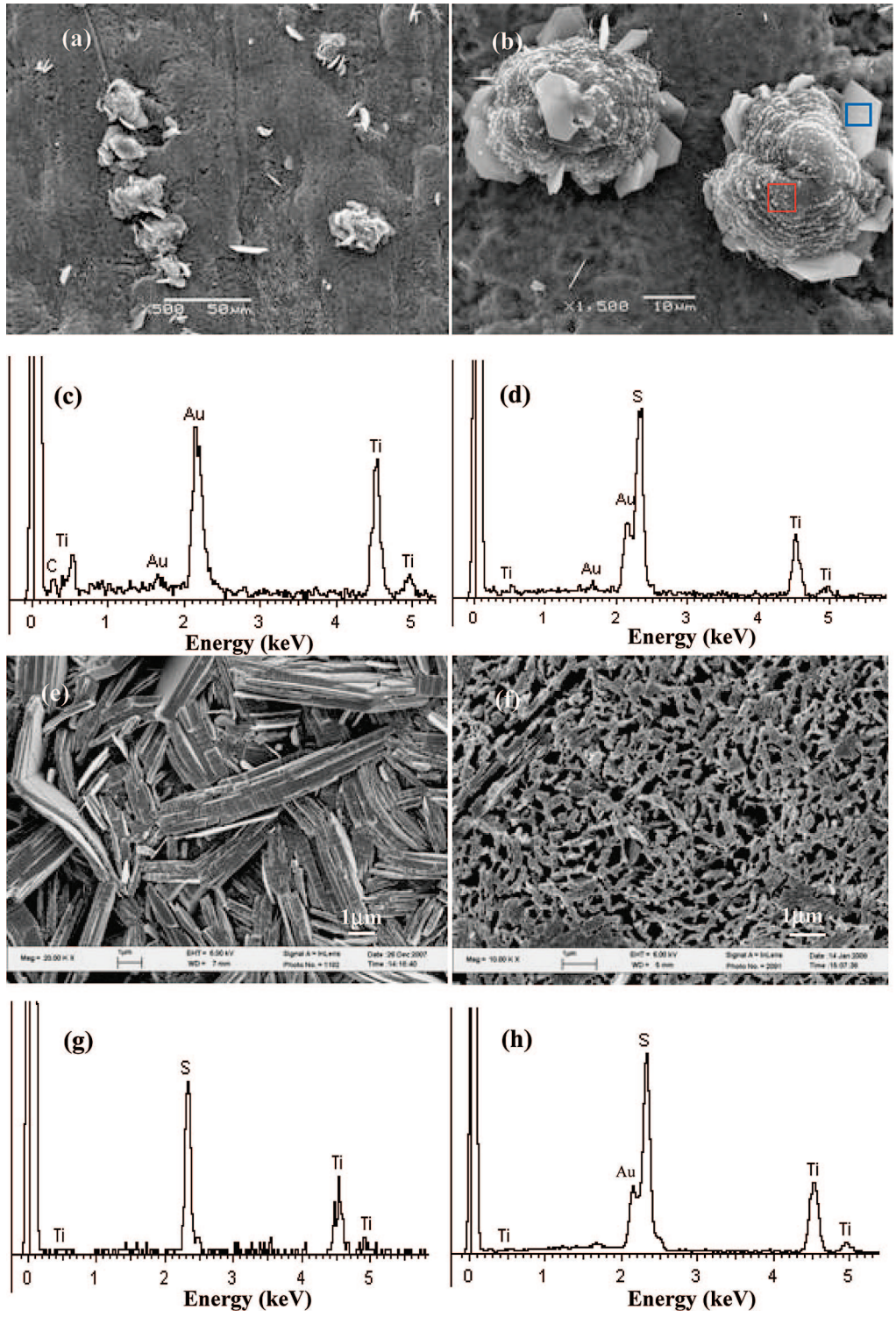

Figure 4. (a, b) SEM images of TiS_2 flower-like patterns prepared at 750 °C (JEOL-JEM-6360LV). EDX spectra of (c) flower center (red box) and (d) flower petal (hexagonal plate) (blue box) prepared at 750 °C. SEM images of (e) TiS_2 microplates prepared at 850 °C and (f) TiS porous films prepared at 950 °C (LEO-1530VP). EDX spectrum of (g) the microplates prepared at 850 °C and (h) the porous films prepared at 950 °C.

vacuum at an applied electric field, and influenced by the microstructures of the material surface.[28] It is well-known that aligned micro/nanostructures with a high packing density can significantly enhance the material FE properties.[29] Because the density of the standing microplates at 550 °C is higher than that of flower-like patterns at 650 °C, the microstructures obtained at 550 °C have a lower turn-on field. The microplates obtained at 850 °C almost overlap so as to lack the tip of the emission electrons, so the microstructures possess the highest turn-on field. However, the values are comparable to the values reported for TaS_2 nanobelts (19.8 V/μm),[30] and vertically aligned SiC nanorods (13−20 V/μm),[31] RuO_2 nanorods (10.3 V/μm),[32] GaN nanowires (12 V/μm),[33] and Si cones (13−16.5 V/μm).[34] Therefore, those microstructures can serve as a novel candidate for future field emitters. Figure 4b displays the corresponding Fowler-Nordheim (FN) plots, that is, the plots of Ln (J/E^2) versus $1/E$. The FN plots of the microstructures exhibit an ap-

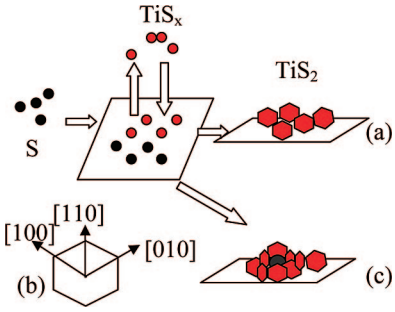

Figure 5. Diagram of formation process of (a) TiS_2 microplates and (c) flower-like patterns. (b) The plane structure of the microplate.

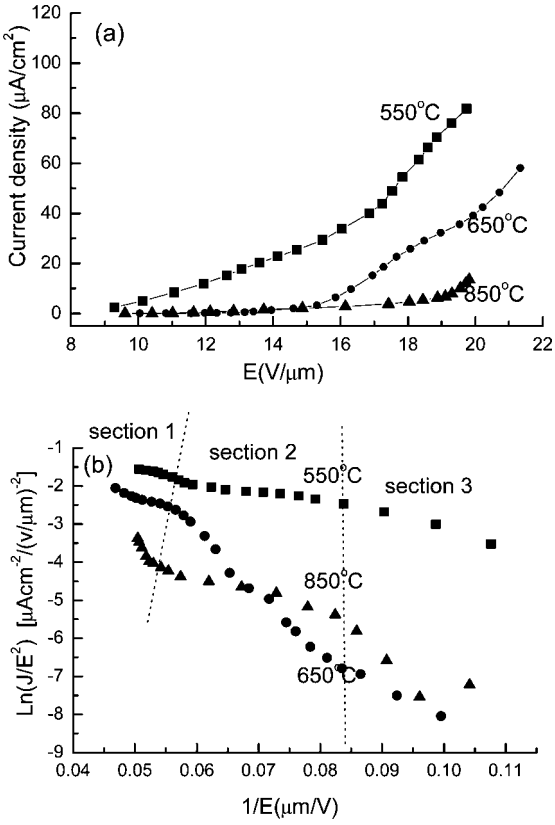

Figure 6. (a) Current density-electric field curves of TiS_2 microstructures obtained at different temperatures and (b) corresponding FN plots.

proximately three-sectional linear behavior, which may result from a space charge effect.[35]

4. Conclusions

TiS_2 microstructures including microplates and flower-like patterns have been fabricated on Ti substrates by a surface-assisted CVT approach. The morphologies of the microstructures strongly depend on the reaction temperature. TiS_2 microplate quasi-arrays formed at 550 °C, whereas the microplates constituted flower-like patterns around Ti particles as a flower center between 650 and 750 °C. The surface of Ti foils was completely converted into standing and overlapping TiS_2 microplates and porous TiS thin films at 850 and 950 °C, respectively. The field emission tests reveal that the microstructures of TiS_2 are electronic field emitters, which can be fabricated into field-emitted devices applied to a microelectronic field.

Acknowledgment. We acknowledge the financial support from the National Science Foundations of China (No. 20671050), and National Basic Research Program of China (973 Program, No. 2007CB936302).

References

(1) Komatsu, S.; Ohta, E.; Tanaka, H.; Moriyoshi, Y.; Nakajima, K.; Chikyo, T.; Shiratani, M. *J. Appl. Phys.* **2007**, *101*, 084904.
(2) Zhou, J.; Xu, N. S.; Deng, S. Z.; Chen, J.; She, J. C.; Wang, Z. L. *Adv. Mater.* **2003**, *15*, 1835.
(3) Huang, M. H.; Mao, S.; Feick, H.; Yan, H.; Wu, Y.; Kind, H.; Weber, E.; Russo, R.; Yang, P. *Science* **2001**, *292*, 1897.
(4) Kusawake, T.; Takahashi, Y.; Yong, W. M.; Ohshima, K. *J. Phys. Condens. Mater.* **2001**, *13*, 9913.
(5) Starnberg, H. I. *Mod. Phys. Lett.* **2000**, *14*, 455.
(6) Reshak, A.H.; Auluck, S. *Phys. Rev. B* **2003**, *68*, 245113.
(7) Shepherd, F. R.; Williams, P. M. *J. Phys. C* **1974**, *7*, 4416.
(8) Chen, C. H.; Fabian, W.; Brown, F. C.; Woo, K. C.; Davies, B.; DeLong, B.; Thompson, A. H. *Phys. Rev. B* **1980**, *21*, 615.
(9) Logothetis, E. M.; Kaiser, W. J.; Kukkonen, C. A.; Faile, S.; Colella, R.; Gambold, J. *Physica B* **1980**, *99*, 193.
(10) Kukkonen, C. A.; Kaiser, W. J.; Logothetis, E. M.; Blumenstock, B.; Schroeder, P. A.; Faile, S. P.; Colella, R.; Gambold, J. *Phys. Rev. B* **1981**, *24*, 1691.
(11) Klipstein, P. C.; Friend, R. H. *J. Phys. C* **1984**, *17*, 2713.
(12) Papageorgopoulos, C. A.; Kamaratos, M.; Papageorgopoulos, D. C.; Tonti, D.; Pettenkofer, C.; Jaegermann, W. *Surf. Sci.* **1999**, *436*, 213.
(13) Takahiro, Y.; Naoshi, S.; Kazuko, M. *J. Phys. C: Solid State Phys.* **1987**, *20*, 395.
(14) Ghorayeb, A. M.; Friend, R. H. *J. Phys. C: Solid State Phys.* **1987**, *20*, 4181.
(15) Whittingham, M. S. *Science* **1976**, *192*, 112.
(16) Whittingham, M. S. *J. Solid Sate Chem.* **1979**, *29*, 303.
(17) Koyano, M.; Negishi, H.; Ueda, Y.; Sasaki, M.; Inoue, M. *Phys. Status Solidi B* **1986**, *138*, 357.
(18) Bardhan, K. K.; Kirczenow, G.; Jackle, G.; Irwin, J. C. *Phys. Rev. B* **1986**, *33*, 4149.
(19) Fujimori, A.; Suga, S.; Negishi, H.; Inoue, M. *Phys. Rev. B* **1988**, *38*, 3676.
(20) Li, D.; Qin, X. Y.; Gu, Y. J. *Mater. Res. Bull.* **2006**, *41*, 282.
(21) Gu, B. L.; Song, Q. G.; Ni, J. *J. Appl. Phys.* **1999**, *85*, 819.
(22) Nath, M.; Rao, C. N. R. *Angew. Chem.* **2002**, *114*, 3601.
(23) Chen, J.; Tao, Z. L.; Li, S. L. *Angew. Chem., Int. Ed.* **2003**, *42*, 2147.
(24) Zhang, Y.; Li, Z. K.; Jia, H. B.; Luo, X. H.; Xu, J.; Zhang, X. H.; Yu, D. P. *J. Cryst. Growth* **2006**, *293*, 124.
(25) Biener, M. M.; Biener, J.; Friend, C. M. *J. Chem. Phys.* **2005**, *122*, 034706.
(26) Wu, X. C.; Hong, J. M.; Han, Z. J.; Tao, Y. R. *Chem. Phys. Lett.* **2003**, *373*, 28.
(27) Fowler, R. H.; Nordheim, L. W. *Proc. R. Soc. London A* **1928**, *119*, 173.
(28) Xu, S. N.; Huq, S. E. *Mater. Sci. Eng. R* **2005**, *48*, 47.
(29) Wang, W. Z.; Zeng, B. Q.; Yang, J.; Poudel, B.; Huang, J. Y.; Naughton, M. J.; Ren, Z. F. *Adv. Mater.* **2006**, *18*, 3275.
(30) Wu, X. C.; Tao, Y. R.; Hu, Y. M.; Song, Y.; Hu, Z.; Zhu, J. J.; Dong, L. *Nanotechnology* **2006**, *17*, 201.
(31) Zhou, X. T.; Lai, H. L.; Peng, H. Y.; Au, F. C. K.; Liao, L. S.; Wang, N.; Bello, I.; Lee, C. S.; Lee, S. T. *Chem. Phys. Lett.* **2000**, *318*, 58.
(32) Cheng, C. L.; Chen, Y. F.; Chen, R. S.; Huang, Y. S. *Appl. Phys. Lett.* **2005**, *86*, 103104.
(33) Chen, C. C.; Yeh, C. C.; Chen, C. H.; Yu, M. Y.; Liu, H. L.; Wu, J. J.; Chen, K. H.; Chen, L. C.; Peng, J. Y.; Chen, Y. F. *J. Am. Chem. Soc.* **2001**, *123*, 2791.
(34) Shang, N. G.; Meng, F. Y.; Au, F. C. K.; Li, Q.; Lee, C. S.; Bello, I.; Lee, S. T. *Adv. Mater.* **2002**, *14*, 1308.
(35) Xu, N. S.; Chen, Y.; Deng, S. Z.; Chen, J.; Ma, X. C.; Wang, E. G. *J. Phys. D: Appl. Phys.* **2001**, *34*, 1597.

CG800113N